Reference Economic Model for Airborne Wind Energy Systems

Joshi, R.; Trevisi, Filippo

DOI
10.5281/zenodo.10959930

Publication date
2024

Document Version
Final published version

Citation (APA)
Joshi, R., & Trevisi, F. (2024). *Reference Economic Model for Airborne Wind Energy Systems*. IEA Wind TCP Task 48. https://doi.org/10.5281/zenodo.10959930

June 2024

IEA Wind TCP Task 48

Tecnical Report

Reference Economic Model for Airborne Wind Energy Systems

iea wind

Reference Economic Model for Airborne Wind Energy Systems

R. Joshi [1] and F. Trevisi [2]

[1] *Delft University of Technology, Delft, The Netherlands.*
[2] *Politecnico di Milano, Milan, Italy.*

June 2024

Technical Report on Cost Modelling, Design Metrics, and Potential Markets

Version 1.0

Airborne Wind Europe TU Delft POLITECNICO MILANO 1863 iea wind

Authors

Rishikesh Joshi
r.joshi@tudelft.nl
Faculty of Aerospace Engineering, Delft University of Technology

Filippo Trevisi
filippo.trevisi@polimi.it
Department of Electronics, Information and Bioengineering, Politecnico di Milano

Acknowledgments

The authors thank Airborne Wind Europe for acting as an intermediary to host the data collection, storage, and dissemination process.

The authors further thank the following people, companies and organisations for their input to this report:

- Kristian Petrick - Airborne Wind Europe
- Roland Schmehl, Dominic von Terzi - Delft University of Technology
- Alessandro Croce, Lorenzo Fagiano - Politecnico di Milano
- Francisco de los Ríos Navarrete, Ivan Castro Fernandez, Gonzalo Sánchez-Arriaga - University Charles III of Madrid
- Wind Fisher
- Rigo Bosman - RIGO Ropes
- Diinef AS
- Marco Ghivarello - GHIVA Progettazione CAD
- Kitepower
- Mozaero
- Florian Stappenbeck (Bauer) - Kitekraft
- Dromec

How to cite

Rishikesh Joshi and Filippo Trevisi (2024) "Reference Economic Model for Airborne Wind Energy Systems" (Version 1). IEA Wind TCP Task 48. https://doi.org/10.5281/zenodo.10959930

You can access the newest version of the report at the link: https://doi.org/10.5281/zenodo.8114627

Code repository

The release of the code linked to this report can be accessed through the link: https://doi.org/10.5281/zenodo.12166697

The latest developments in the code can be accessed at: https://github.com/awegroup/AWE-Eco

Funding

This work has been partially supported by the MERIDIONAL project, which receives funding from the European Union's Horizon Europe Programme under the grant agreement No. 101084216.

This work has been partially funded by the NEON research program and has received funding from the Dutch Research Council NWO under the grant agreement No. 17628.

Preface

Becoming one of the most cost-efficient renewable energy technologies is one of the big goals of the airborne wind energy sector. Airborne wind energy systems (AWESs) are not yet at the same cost level as established renewable energy technologies, therefore, a transparent cost basis for AWESs is crucial in order to allow stakeholders to make informed decisions: policymakers require reliable cost models to base upon their decisions on potential support schemes; clients and investors need to understand where cost savings are possible when scaling up the production of AWESs; and AWE developers need to benchmark their systems both within and outside the AWE sector - and being able to compare costs will also help them identify opportunities for joint purchasing initiatives or other ways of collaboration. This reference economic model aims to set a baseline of current AWES costs and allow tracking cost developments for the future, thus providing a solid basis for decision-makers. It is aligned with methodologies used by international organisations such as the IEA or IRENA. In short, this model will help the AWE sector gain recognition and advance towards a prosperous future.

Kristian Petrick
Secretary General, Airborne Wind Europe
Brussels, May 2024

Summary

This work falls under the IEA Wind Task 48 activity and is the result of a collaborative effort between industry and academia. Airborne Wind Europe facilitated the setup of this work and acts as an intermediary for data collection, storage, and dissemination.

This technical report and the developed computer code provide parametric cost models that aim to estimate both capital expenditure (CapEx) and operational expenditure (OpEx) associated with each component of airborne wind energy systems (AWESs). Furthermore, the report identifies relevant design metrics that could be used as objectives for the optimisation and refinement of AWES designs. These metrics will not only aid in evaluating the performance and efficiency of AWESs but will also guide future research and development efforts. In addition to cost modelling and design metrics, the report delves into potential markets where AWESs could play a significant role in the global energy supply mix.

This report aims to be a valuable resource for researchers, industry and policy makers who want to understand the economic aspects, design considerations and market potential of AWESs. It sets the groundwork for informed decision making, road mapping of technology development, and collaborative efforts to advance the adoption and deployment of AWESs on a global scale.

Contents

1 Introduction

Airborne wind energy (AWE) refers to the field of wind energy in which tethered flying systems are used to harvest wind power at potentially higher altitudes. Airborne wind energy systems (AWESs) can be classified in different ways. A popular classification criterion is the type of flight operation, which can be crosswind or tether-aligned. Crosswind AWESs, which are considered in this report, use kites flying perpendicular to the wind direction. Other frequently used criteria are related to the power generation method. In the ground generation (GG) concept, the kite pulls the tether and unwinds a generator placed on the ground. In the rotational concept, the torque generated by a network of wings is transmitted to a generator placed on the ground via network of tethers. In the fly generation (FG) concept, power is generated onboard with small wind turbines. Another type of classification is based on the type of the flying device, for which a number of variants exist (soft-wing, fixed-wing, hybrid-wing etc.).

More details on the various concepts, that are pursued by active companies, research institutions and the sector status are provided in [1].

1.1 Objective

The objective of this work is the cost modelling, the definition of design metrics that could be used as design objectives, and the description of potential markets for AWESs. These aspects are necessary to understand the economic potential of AWE and are crucial when designing a system for a given application. A reference economic model is useful both for industry and for academia. Industry can use it to assess the economic viability of their specific implementation while ensuring the economic properties are aligned with the respective information of competitors. Academics can use it to assess economic aspects of their research, while ensuring that this information was derived from up-to-date industry data.

The economic model described in this report is also provided as a computer code [2] which can be used to perform techno-economic analyses, system design optimisation studies, and to evaluate business cases for specific market scenarios. Figure 1 summarises the purpose and the use case of the model. It can be used to estimate the economic performance for given system and site specifications, if combined with a performance model. The generated results can assist in the development of technology roadmaps and inform policy makers and organisations such as International Renewable Energy Agency (IRENA) or International Energy Agency (IEA).

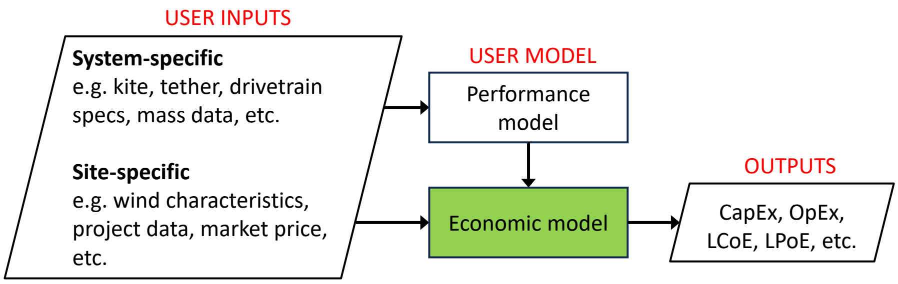

Figure 1: Flowchart representing the inputs and outputs of the developed economic model.

1.2 Methodology

The IEA Wind Task 48 [3] aims at building a strong collaborative for accelerating the development and commercialisation of AWE technology. This work falls under Work Package 1, which focusses a.o. on identifying economic drivers and the potential of deploying AWE in different markets. Building, refining, and validating this economic model must be a collaborative effort between academia and industry to ensure high quality. The process of developing this reference economic model is shown in Fig. 2. A workshop was conducted as an IEA Wind Task 48 activity in June 2023 for the introduction and call for collaboration on this work. The workshop was attended by the AWE industry and academic institutions. Around 17 participants expressed interest and of those 10 participants were able to provide significant inputs within the planned timeframe. The portfolio of participants who provided input includes AWE companies, tether and ground station manufacturers, suppliers, and university research groups.

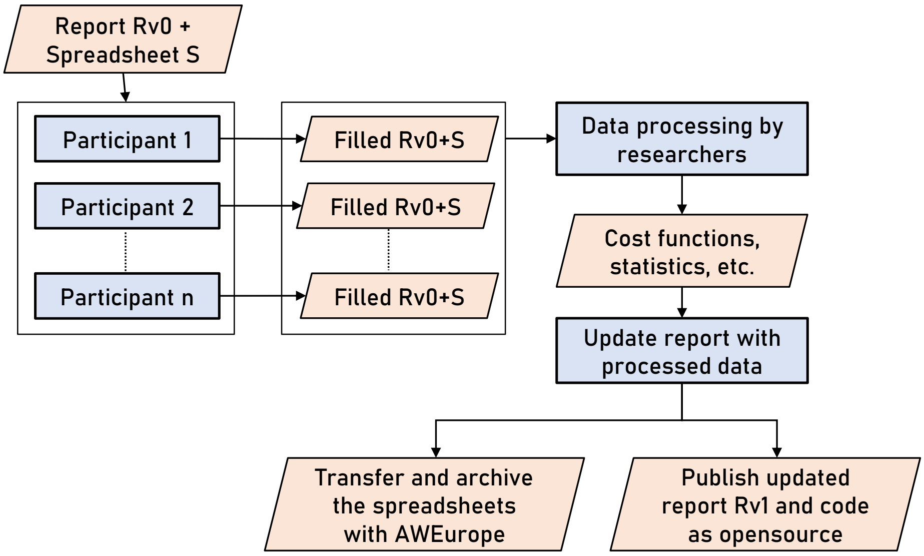

Figure 2: Flowchart showing the adopted process to build the reference economic model for airborne wind energy systems. Here, 'Rv0' corresponds to the *version 0* of the report and 'S' corresponds to the individual spreadhseet provided to the participants.

The primary aspect of the economic model is the cost modelling of different concepts. The initial formulation of cost functions that are dependent on key design parameters such as kite wing area, span, aspect ratio, tether properties, generator characteristics, etc. was described in the *version 0* of this report. This initial version was provided to participants along with individual spreadsheets to collect their feedback and inputs. These data have been used to update the cost functions and produce the present (*version 1*) of the report. The cost model is implemented as a modular code in MATLAB. This updated report (https://doi.org/10.5281/zenodo.8114627) and the code (https://github.com/awegroup/AWE-Eco) are published opensource and the individual spreadsheets are archived with Airborne Wind Europe to preserve anonymity. Airborne Wind Europe acted as an intermediary to host the data collection, storage and dissemination.

In addition to the input of the workshop participants, publicly available reports and articles were also used to collect cost references. Table 1 lists the relevant literature available on the cost modelling of AWESs and wind turbines which is referred to in this report.

Table 2 lists the relevant literature available on the design metrics of AWESs and wind turbines which is referred to in this report.

By their nature, cost models are highly uncertain because they are subject to nonscientific, nontechnical, site-dependent, and sometimes political considerations. Therefore, many assumptions must be considered in the derivation, especially at the current early stage of technology development. The cost references provided in this report are based on the early commercialisation of AWESs with the system sizes ranging from 100 kW-2 MW, and series production volumes of 50+ units. The costs are not based on significant effects of economies of scale. Moreover, we do not consider any overhead costs in development, manufacturing and profit margins which might be significant for certain low TRL (Technology Readiness Level) and CRL (Commercial Readiness Level) components.

These assumptions are taken to identify each sub-system's cost driver, and model the related cost dependencies. Different AWE concepts have different designs, and thus different economic performances are expected. To provide a consistent way to evaluate the economic performance of different AWE concepts,

Table 1: Referenced literature for cost modelling.

Year	Authors	Focus	Citation
2013	J. Heilmann, C. Houle	GG soft-wing	[4]
2014	C. Grete	GG soft-wing	[5]
2016	M. De Lellis et al.	GG soft-wing	[6]
2018	P. Faggiani, R. Schmehl	GG soft-wing	[7]
2018	F. Bauer et al.	FG fixed-wing	[8]
2019	BVG Associates	Conventional WTs	[9]
2019	NREL	Conventional WTs	[10]
2019	M. Garcia-Sanz	Conventional WTs and AWESs	[11]
2020	N. Tucker	FG fixed-wing	[12]
2020	F. Trevisi et al.	GG & FG fixed-wing	[13]
2021	NREL	Conventional WTs	[14]
2022	BVG Associates	GG & FG	[15]
2022	NREL	PV & BESS	[16]

Table 2: Referenced literature for design metrics.

Year	Authors	Focus	Citation
2016	L. Hirth, S. Müller	Value metric	[17]
2020	J. Simpson et al.	Value metric	[18]
2022	H. Canet et al.	LCA metric	[19]
2023	R. Joshi et al.	Profit metric	[20]

this report and the included model have been developed to be as general as possible. This cost model aims at being generic and comprehensive of all the AWE concepts. However, due to the lack of data, this version is developed for GG and FG crosswind AWESs, with soft or fixed wings. The fixed-wing kites are expensive but last longer, while the soft-wing are less expensive but need to be replaced more frequently. This shifts costs from initial investment to operational expenditure. Such trade-offs could be captured by using this model.

How to contribute

This entire process needs to be repeated periodically, to keep the report up-to-date with the development of the sector. Therefore, the authors call for new researchers to help in the development of future versions of this report. To initiate the next version, please contact Airborne Wind Europe [1].

1.3 Outline

The terminology and nomenclature used is aligned with the published glossary in [1]. The report is organised into three main parts:

1. Cost modelling. For every component and subcomponent of the AWES as shown in Figure 3, the total costs are divided into capital expenditure (CapEx) and operational expenditure (OpEx). This part is divided into the following sections:

    - Section 2: Cost model of the kite and its subcomponents;
    - Section 3: Cost model of the tether;
    - Section 4: Cost model of the ground station and its subcomponents;

- Section 5: Cost model of the balance of system;
- Section 6: Description of balance of plant;

2. Definition of design metrics (Section 7);
3. Description of potential markets (Section 8).

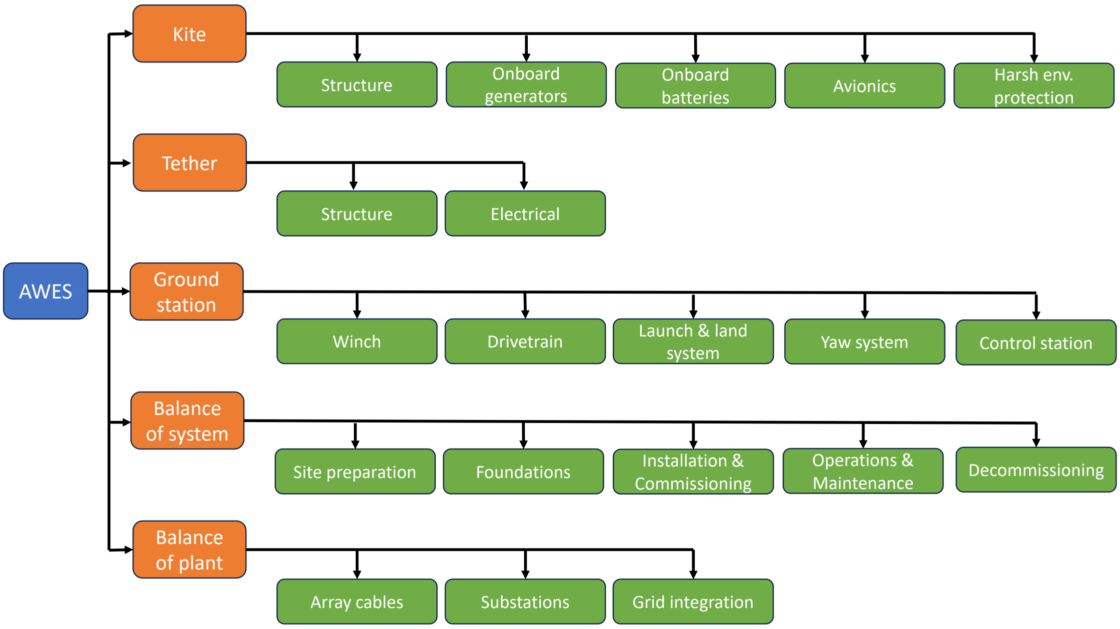

Figure 3: Breakdown of cost components of an airborne wind energy system used in this report. The system is represented in 'blue', the components in 'orange', and the subcomponents in 'green'.

Figure 4 shows the used classification of components and subcomponents applied to an existing system from [21].

Nomenclature in the code

All the titles of the sections, subsections, and sub-subsections in the main text have keywords in the brackets that denote the corresponding nomenclature used in the provided code. The component naming concept is based on a hierarchical subdivision of the AWESs. The separation by a dot means that the second component is a child of the first component, and so on.

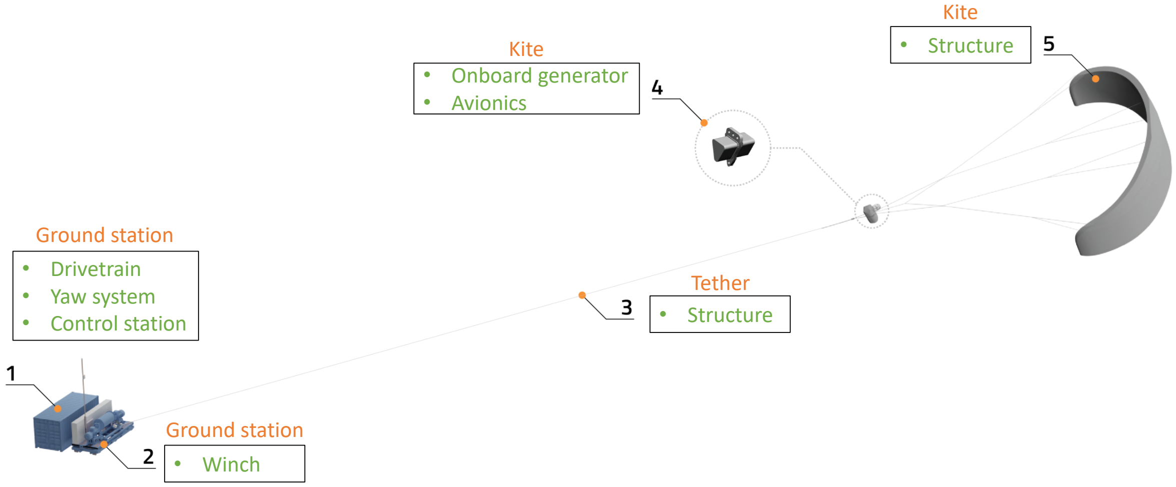

Figure 4: Subcomponents classification used in the report as applied to an existing system. Image from [21]. Note that not all subcomponents are necessarily a part of every system.

2 Kite (kite)

The flying subcomponents are responsible for converting the wind power into mechanical power and thus their cost models play a central role in this report. Currently, many different kite concepts are being explored in airborne wind energy, increasing the complexity of a comprehensive cost model. Indeed, different kite designs lead to different technical implementations and thus costs. In this report, the most researched concepts in airborne wind energy are modelled. These are GG AWESs based on soft and fixed wings and FG AWESs. The cost modelling of the flying components of less common concepts (e.g. Rotational, Magnus effect, etc.) is left for future versions of this report.

2.1 Structure (kite.structure)

In this section, the cost models for the kite structure are developed. For GG AWESs, the kite can be based on a soft or fixed wing. Structural costs are expected to drop with the technology developing further and with improved structural designs. Future versions of this report might show this decrease.

2.1.1 Fixed-wing kites (kite.structure.fixed)

Fixed wings can be used for GG and FG AWESs. Two approaches for the cost model of the structural material are introduced here. The first model is a simplified model which computes the cost based on the total wing mass. The second model provides only the cost of the materials that could be used in a detailed design process.

CapEx approach 1 (kite.structure.fixed.one.capex)

The kite structure cost is assumed proportional to the kite's structural mass m_{str} and wing area. The dependence on the mass is due to the costs of composite material, adhesive, and production. The dependence on the wing area is due to the costs of surface treatment, coating etc. The costs are modelled as

$$C_{\mathrm{str}} = p_{\mathrm{str}} m_{\mathrm{str}} + p_{\mathrm{wet}} S_{\mathrm{wet}}, \tag{1}$$

where S_{wet} is wetted area. The wetted area refers to the total surface area of the kite that is in contact with the air when it's flying. This includes the wings, fuselage, tail surfaces, and any other parts that are exposed to the airflow during flight. p_{str} is in € kg^{-1} and p_{wet} is in € m^{-2}. The cost references are in Table 3.

Table 3: Cost references for kite structure costs.

Parameter	Value	Units
p_{str}	250	€ kg^{-1}
p_{wet}	200	€ m^{-2}

If a good estimate of the structural mass is not available, it can be estimated based on AWESs prototypes as a function of the wing span b [22]

$$m_{\mathrm{str}} = m_{\mathrm{ref}} \left(\frac{b}{b_{\mathrm{ref}}} \right)^3, \tag{2}$$

taking $m_{\mathrm{ref}} = 36.8$ kg and $b_{\mathrm{ref}} = 5.5$ m. This expression can be used as a first guess for the estimation of the total mass and should be used with care.

CapEx approach 2 (kite.structure.fixed.two.capex)

The second cost model for the structural mass requires a preliminary structural design. The structural design can be based on the fibreglass composite materials in Table 4, for which the material costs are provided. Manufacturing and tooling costs could represent a large share of the total structural cost. They can be estimated in a simplified way by applying the factor $f_{\mathrm{man}} = 0.75$ to the total cost of the material.

Table 4: Material Data: Uniax and Triax glass fiber composite material.

Parameter	Uniax	Triax	Units	Description
E_1	41.6	21.8	GPa	Young's modulus in 1-direction
E_2	14.9	14.7	GPa	Young's modulus in 2-direction
G_{12}	5.0	9.4	GPa	In-plane shear modulus
ν_{12}	0.28	0.45	-	Poisson ratio 12
ρ	1950	1845	$\mathrm{kg\,m^{-3}}$	Mass density
p_{gl}	3	3.6	€ $\mathrm{kg^{-1}}$	Material price

OpEx (kite.structure.fixed.opex)

Not modelled due to lack of information and data.

2.1.2 Soft-wing kites (kite.structure.soft)

Soft kites, also known as soft wings, have flexible structures made of lightweight materials such as nylon, polyester (Dacron) or polyethylene (Dyneema) fabric. This flexibility allows them to be easily manoeuvred and controlled in the air. The structure costs include the costs of the fabric (including reinforcements) and the bridle lines.

CapEx (kite.structure.soft.capex)

The flat wing area A is estimated from the projected area S with $A = (25/18)S$. The aspect ratio is assumed to not influence the wing cost and the influence of the wing design and type on the cost is neglected. The total costs are estimated to be a function of the wing area as

$$C_{\mathrm{str}} = (p_{\mathrm{fabric}} + p_{\mathrm{bridle}})A, \tag{3}$$

where $p_{\mathrm{fabric}} = 45$ € $\mathrm{m^{-2}}$ and $p_{\mathrm{bridle}} = 8$ € $\mathrm{m^{-2}}$.

OpEx (kite.structure.soft.opex)

The lifetime of the kite is necessary information to estimate the replacement costs. If a good estimate of the kite lifetime is not available, it can be assumed to be of $L_{\mathrm{str,soft}} = 5000$ flying hours at full loading (i.e., maximum tether force), which corresponds to $L_{\mathrm{str,soft}} = 0.57$ flying years.

To estimate the how much of the kite lifetime has been used, one can find the equivalent used lifetime knowing the wind distribution $f(v_{\mathrm{w}})$ (e.g. Weibull) and the tether force, which approximates the loading on the kite, as a function of wind speed $F_\mathrm{t}(v_\mathrm{w})$. To find the equivalent used lifetime, we define the Loading Factor LF as

$$LF = \int_{v_\mathrm{in}}^{v_\mathrm{out}} f(v_\mathrm{w}) \frac{F_\mathrm{t}(v_\mathrm{w})}{F_\mathrm{t,max}} \mathrm{d}v_\mathrm{w}, \tag{4}$$

where v_in and v_out are the cut-in and the cut-out wind speed respectively. The frequency of replacements per year is then $f_\mathrm{repl,str} = \frac{LF}{L_\mathrm{str,soft}}$.

2.2 Onboard Generators (kite.obgen)

FG AWESs use the onboard generators for take-off, power generation, and land which then represents a significant cost. Instead, GG AWESs typically generate a small amount of power onboard, which is needed to power the onboard avionics. Except soft-wing systems, the GG AWESs typically use these generators as motors for take-off and land. They can also be used during the power generation phase to enhance control authority.

CapEx (kite.obgen.capex)

The onboard generator cost can be expressed as a function of their rated power as

$$C_\mathrm{ob,gen} = p_\mathrm{ob,gen} P_\mathrm{rated,ob,gen}, \tag{5}$$

where $p_\mathrm{ob,gen} = 120$ € kW^{-1} and $P_\mathrm{rated,ob,gen}$ is in kW.

OpEx (kite.obgen.opex)

Not modelled due to lack of information and data.

2.3 Onboard Batteries (kite.obBatt)

The onboard batteries are used to supply power to the avionics and the onboard generators when needed. The sizing of these batteries depends on the amount of energy required by the onboard systems.

CapEx (kite.obBatt.capex)

The cost of the batteries is estimated to be proportional to the batteries' capacity. The costs are $p_\mathrm{ob,batt} = 150$ € $\mathrm{kW}^{-1}\,\mathrm{h}^{-1}$.

OpEx (kite.obBatt.opex)

Not modelled due to lack of information and data.

2.4 Avionics (kite.avionics)

The avionics, also know as the kite control unit or the control pod, typically includes all the electronic systems used on aircraft, such as communication and navigation hardware, sensors, CPUs, and any electronic system needed to perform individual functions.

CapEx (kite.avionics.capex)

Avionics cost is modelled as a fixed cost, not dependent on the size of the AWESs. According to the required sensors, electronics and computational power, the cost can vary significantly. Moreover, the avionics cost for series production is expected to increase with respect to prototype cost because of the aviation grade certification and required redundancy.

For prototypes, the avionics cost can be estimated to be $C_{\text{avio}} = 15$ k€.

For early series production, the aviation certification and the redundancy requirements are expected to raise the cost of soft-wing kite systems to $C_{\text{avio}} = 30$ k€ and of fixed-wing kite systems to $C_{\text{avio}} = 150$ k€.

OpEx (kite.avionics.opex)

Not modelled due to lack of information and data.

2.5 Tether attachment (kite.tAttach)

Not modelled due to lack of information and data.

2.6 Harsh environment protection (kite.protection)

Not modelled due to lack of information and data. This component involves all the protection equipment necessary in extreme events or to ensure longer life. Among others, these might include

- Lightening protections;
- Ground or in-flight deicing protection;
- Leading-edge erosion protection;
- Emergency landing apparatus.

3 Tether (tether)

The tether connects the kite to the ground station. For GG systems, the tether is a structural component which has to withstand the pulling force of the kite, whereas for FG systems, it is also a electrical component responsible to transmit the generated electricity to the ground station.

CapEx (tether.capex)

For GG, the tether cost scales with the total mass of the tether. The price in € kg^{-1} depends on the type of material and the suppliers. The tether fibre commonly used in the AWE industry is the Dyneema DM20 fibre [23], arranged in 12 strand braided tethers and manufactured such that the tethers are hollow and have inner room for a core. This hollow core can contain cables for power or signal transfer. The nominal diameters are measured on new tethers, which however decrease in diameter after some loading is applied (see difference between *Nominal diameter* and *Worked-in diameter* in Table 33.4 of [23]). The worked-in (i.e. reduced) diameter needs to be used in AWE performance studies. An additional mass to the fibre mass needs to be taken into account for the coating (coating content $f_{\text{coat,t}} \approx 0.1$ of the total tether mass). The tension on the fibre σ_t, which is the quantity needed to estimate the compliance with respect to the material strength $\hat{\sigma}_\text{t}$ and the tether life, can be estimated based on the fibre density $\rho_\text{t} = 970\,\text{kg}\,\text{m}^{-3}$ and on the fibre linear weight (given in Table 33.4 of [23]) as

$$\sigma_\text{t} = \frac{F_\text{t}\,[\text{N}]\cdot\rho_\text{t}\left[\text{kg/m}^3\right]}{\text{fibre linear weight [kg/m]}} = \frac{F_\text{t}\,[\text{N}]\cdot\rho_\text{t}\left[\text{kg/m}^3\right]}{(1-f_{\text{coat,t}})\cdot\text{ tether linear weight [kg/m]}}, \tag{6}$$

where F_t is the force applied to the tether.

If no detailed information about the tether design is available, a hollow core of 15 % the cross-sectional area can be assumed, such that the stress acting on the fibre can be approximated with

$$\sigma_\text{t} \approx \frac{F_\text{t}}{f_\text{At}\cdot\pi\frac{d_\text{t}^2}{4}}, \tag{7}$$

where d_t is the worked-in tether diameter, which is used in performance models, and $f_\text{At} \approx 0.85$ is the ratio between the cross-sectional area taken by the fibres and the tether cross-sectional area.

A detailed discussion on tether design, typically carried out to ensure a given working life, is beyond the scope of this report and can be found at [23].

An approximate price of this type of tethers, which need special coating treatments for improved bending, is $p_\text{t} = 80$ € kg^{-1}, such that the tether cost is

$$C_\text{t} = p_\text{t} m_\text{t}, \tag{8}$$

where m_t is the total tether mass.

For FG, the tether comprises a structural and an electrical part. The electric conductors are assumed to have a negligible material price compared to the structural part, but the dedicated manufacturing largely influence the tether cost. The cost of such a rope can be modelled by applying a manufacturing factor $f_{\text{m,t}}= 2.5$ to the tether cost estimated for GG AWESs.

OpEx (tether.opex)

Bosman et al. [23] describes the design drivers for the tether and highlight that bending fatigue and creep as the leading causes of tether failure.

The bending fatigue is mainly relevant for GG systems since it arises when the tether is wound around the winch with high tension. The tether life due to bending mainly depends on the ratio between the winch diameter and the tether diameter. The life due to bending is estimated using the method described in [23].

The number of cycles to failure N_{b} is function of the ratio between the winch diameter and the tether diameter (i.e. $d_{\mathrm{winch}}/d_{\mathrm{t}}$) and the winding tension. It can be approximated with

$$N_{\mathrm{b}}(\sigma_{\mathrm{t}}) = 10^{(a_{1,\mathrm{b}} - a_{2,\mathrm{b}}\sigma_{\mathrm{t}})}, \quad \text{for range,} \quad 0.2 < \sigma_{\mathrm{t}} < 0.8 \text{ GPa}, \tag{9}$$

where σ_{t} is in GPa and the values of $a_{1,\mathrm{b}}$ and $a_{2,\mathrm{b}}$ are given in Table 5.

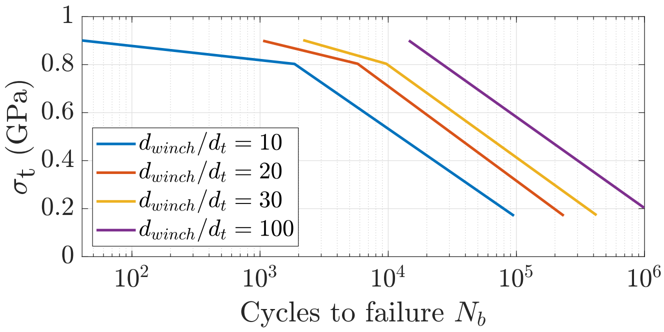

Figure 5: Bending fatigue performances of SK75 with DSM proprietary coating [23].

Table 5: Parameters $a_{1,\mathrm{b}}$ and $a_{2,\mathrm{b}}$ (Eq. 9) as a function of the ratio between the winch diameter and the tether diameter $d_{\mathrm{winch}}/d_{\mathrm{t}}$ of SK75 with DSM proprietary coating.

$\mathbf{d}_{\mathrm{winch}}/\mathbf{d}_{\mathrm{t}}$	10	20	30	100
$\mathbf{a}_{1,\mathrm{b}}$	5.4	5.8	6.1	6.5
$\mathbf{a}_{2,\mathrm{b}}$		2.6		

To estimate the tether life due to bending fatique, the number of bends for cycle N_{bends} (i.e. the number of pulleys) and the time per cycle as a function of wind speed $\Delta t_{\mathrm{cycle}}(v_{\mathrm{w}})$ is needed. Using the Miner's rule, for a given a wind distribution $f(v_{\mathrm{w}})$, a tether failure will occur when

$$L_{\mathrm{t,bend}} N_{\mathrm{bends}} \int_{v_{\mathrm{in}}}^{v_{\mathrm{out}}} \frac{f(v_{\mathrm{w}})}{\Delta t_{\mathrm{cycle}}(v_{\mathrm{w}}) N_b(\sigma_{\mathrm{t}}(v_{\mathrm{w}}))} \mathrm{d}v_{\mathrm{w}} = 1, \tag{10}$$

where $L_{\mathrm{t,bend}}$ is the tether life and thus the frequency of tether replacement is $f_{\mathrm{bend}} = \frac{1}{L_{\mathrm{t,bend}}}$. If no detailed information about the the time per cycle is available, one can assume $\Delta t_{\mathrm{cycle}}(v_{\mathrm{w}}) = 60$ s. Improving the fibre types and the construction can enhance the lifetime considering by a factor up to 6 [23].

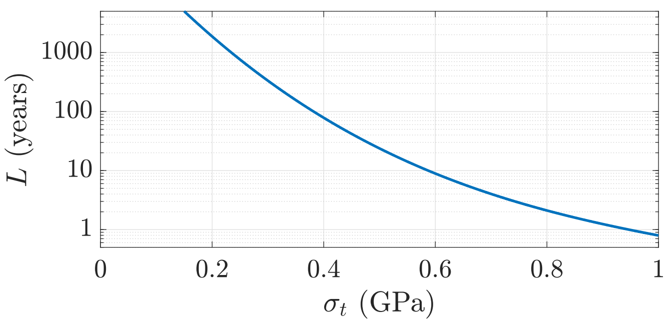

Figure 6: Safe working life (T= 20 °C) graphs for DM20 Dyneema fibre based on creep rupture [23].

Failure due to creep is more relevant for FG systems than failure due to bending. The creep curve shown in Fig. 6 represents the tether life $L(\sigma_{\mathrm{t}}(v_{\mathrm{w}}))$ in logarithmic scale if only a given stress level $\sigma_{\mathrm{t}}(v_{\mathrm{w}})$ was applied. A polynomial approximation in the linear scale of the tether life curve for the highest-performing rope DM20 is

$$L(\sigma_t) = 10\hat{}\left(-2.4\sigma_{\mathrm{t}}^3 + 8.3\sigma_{\mathrm{t}}^2 - 11.2\sigma_{\mathrm{t}} + 5.2\right), \tag{11}$$

where σ_{t} is in GPa.

Given a wind distribution $f(v_{\mathrm{w}})$, a tether failure occurs when

$$L_{\mathrm{t,creep}} \int_{v_{\mathrm{in}}}^{v_{\mathrm{out}}} \frac{f(v_{\mathrm{w}})}{L(\sigma_{\mathrm{t}}(v_{\mathrm{w}}))} \mathrm{d}v_{\mathrm{w}} = 1. \tag{12}$$

The frequency of tether replacement per year is $f_{\mathrm{t}} = \frac{1}{L_{\mathrm{t,creep}}}$. Note that some correction factors could be applied to account for the low tension during the reel-in phase and for the change in temperature during the day and during the seasons [23].

4 Ground station (gStation)

The specific components of the ground station will vary depending on the different concepts of the AWESs. For GG systems, the ground station consists of 1) the winch, which supports the loads during operation and stores the tether; 2) the drivetrain, which transfers and converts the mechanical power to electrical power; 3) the yawing mechanism, which enables the kite to align with the wind direction; 4) the launch and land system; 5) the control and communications unit. For FG systems, the drivetrain will not include the generator. The functions of other components remain more or less the same.

The power production profiles of AWESs are oscillating by nature. AWESs need to smoothen their power output to comply with grid codes before they can be connected to the respective electricity grids. This smoothing of the power could be achieved by using intermediate storage components that act as buffers to charge and discharge during the operation. Three different types of drivetrain configurations depending on different storage solutions were explored in [24]. This report considers the Electrical and the Hydraulic drivetrains in detail. Some other innovative drivetrain solutions exist, such as a linear generator, as described in [25]. Another approach to achieve farm-level power smoothing is to operate multiple AWESs in a phase-shifted but synchronised manner. Although it is expected to reduce the requirement of the intermediate storage solution, it will be a challenging control problem that could be tackled in the future.

The following subsections describe the cost modelling of each of these ground station components.

4.1 Winch (gStation.winch)

For GG AWESs, the winch is the component of the ground station on which the tether is spooled during operation. This component translates the pulling force of the tether in the form of rotational power input to the drivetrain. In principle, it is a hollow cylinder with a certain thickness. The costs for control and winding mechanisms including pulleys, guide rails etc, are not considered.

For FG AWESs, the winch is the component of the ground station on which the tether is winded when the system is not operating.

CapEx (gStation.winch.capex)

The cost of the winch is assumed to scale with its own mass [26]. The winch could be typically made of aluminium or steel. Data on these materials are listed in Table 6. The winch mass can be computed using the tether diameter as the rolling pitch. A safety margin of around 10% is generally used on the tether diameter to calculate the pitch. The winch will also have some dead windings which are not used. Hence, a safety factor on the tether length must also be applied. The winch mass is computed as

$$m_{\text{winch}} = \frac{\pi \left(d_{\text{winch}}^2 - (d_{\text{winch}} - 2t_{\text{winch}})^2\right)}{4} \frac{l_{\text{t}} SF_{\text{l}_\text{t}}}{\pi d_{\text{winch}}} \, d_{\text{t}} SF_{\text{d}_\text{t}} \, \rho_{\text{mat}}, \tag{13}$$

where d_{winch} is the external winch diameter, t_{winch} its thickness, d_{t} the tether diameter, SF_{d_t} is the safety margin on tether diameter, l_{t} the tether length, SF_{l_t} is the safety margin on tether length, and ρ_{mat} the material density (e.g. aluminium or steel). The first fraction represents the cross-sectional area, the second represents the number of windings of the tether around the winch, the third represents how much axial space is needed for each winding, and the last term is the material density.

For GG AWESs, the winch can be designed with the following methodology, if no other information are available. The maximum tether force $F_{\text{t,max}} = \hat{\sigma}_{\text{t}} \frac{\pi d_{\text{t}}^2}{4}$, where $\hat{\sigma}_{\text{t}} = 1.5$ GPa is the tether fibre (Dyneema DM20) strength, assuming no hollow core in this section. We assume that the winch should withstand the same force, distributed over a rectangular area of width d_{t} and height t_{winch} i.e. $F_{\text{t,max}} = \hat{\sigma}_{\text{mat}} d_{\text{t}} t_{\text{winch}}$, where $\hat{\sigma}_{\text{mat}}$ is the strength of the winch material. Therefore, the winch thickness can be correlated to the tether diameter as

$$t_{\text{winch}} = \frac{\pi \hat{\sigma}_{\text{t}}}{4\hat{\sigma}_{\text{mat}}} d_{\text{t}}. \tag{14}$$

Table 6: Winch related data. Material 1 is aluminium, while material 2 is steel.

	Parameter	Value	Units
mat. 1	p_{al}	10	€kg^{-1}
	ρ_{al}	2700	$\mathrm{kg\,m^{-3}}$
	$\hat{\sigma}_{\mathrm{al}}$	300	MPa
mat. 2	p_{st}	7	€kg^{-1}
	ρ_{st}	7850	$\mathrm{kg\,m^{-3}}$
	$\hat{\sigma}_{\mathrm{st}}$	500	MPa
	$d_{\mathrm{winch}}/d_{\mathrm{t}}$	50	-
	$SF_{\mathrm{d_t}}$	1.1	-
	$SF_{\mathrm{l_t}}$	1.1	-

Since this is a simplified method, it ignores the effects such as the force distribution over the entire winch, stress concentrations, and dynamic loading. An additional safety factor of 2 could be applied to the estimated thickness of the winch to account for the ignored effects.

For FG AWESs, the winch is responsible of storing the tether when the system is not producing power. Therefore, the thickness can be assumed to be equal to the tether diameter $t_{\mathrm{winch}} = d_{\mathrm{t}}$, if no other information are available.

OpEx (gStation.winch.opex)

Not modelled due to lack of information and data.

4.2 Electrical drivetrain (drivetrain_type=1)

The drivetrain is fundamentally different for FG and GG systems since for FG systems the generator is onboard and for GG systems it is on the ground. Based on the commercial readiness and proven track-record of comprising components, the more suitable drivetrain for market entry is expected to be the electrical drivetrain, as shown in Figure 7. For GG systems, the generator is directly connected to the winch with or without a gearbox. During cycle operation throughout the windspeed range, the speed and torque of the winch varies within a wide range. Hence a gearbox could be necessary to translate the winch's speed and torque values within the operational range of the generator. A gearbox could be excluded if the generator is custom designed according to the operation of the AWES. The generator is connected to an electrical storage and the grid via power converters. The storage solution has to be charged and discharged during the cycle to maintain a smooth power output at the grid side.

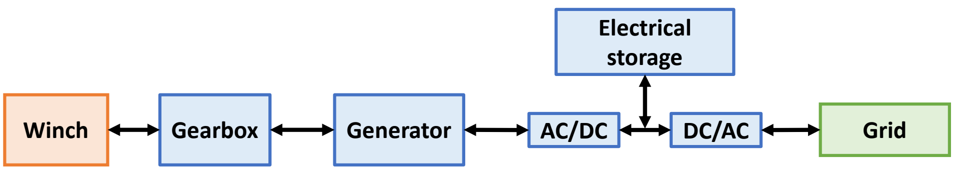

Figure 7: Electrical drivetrain architecture (adapted from [24]).

FG systems have the generators onboard but they would still require the intermediate storage on the ground for power smoothing.

4.2.1 Gearbox (gStation.gearbox)

Since the generator is connected to the winch using the gearbox, it has to be sized for the peak mechanical loading during the reel-out phase. The cost and size of the gearbox is not only driven by power, but also by torque. The benefit of using a gearbox could be to reduce generator costs by controlling the input speed and torque of the generator. Though scaling the gearbox costs by torque will give better estimates, due to availability of data, we model the costs with power.

CapEx approach 1 (gStation.gearbox.one.capex)

The costs are modelled as

$$C_{\text{gb}} = p_{1,\text{gb}} P_{\text{rated,gb}}, \tag{15}$$

where p_{gb}=70 € kW^{-1} and $P_{\text{rated,gb}}$ is the peak input mechanical power to the gearbox.

As a probable ballpark value, this peak mechanical input power could be 2.5 times the electrical rated power for GG systems.

CapEx approach 2 (gStation.gearbox.two.capex)

Gearbox costs can be modelled similarly to as modelled for conventional wind turbines. The cost functions used in the WISDEM tool by NREL [10] are as follows:

$$m_{\text{gb}} = k_{1,\text{gb}} \tau^{b_{\text{gb}}} \tag{16}$$

$$C_{\text{gb}} = p_{2,\text{gb}} m_{\text{gb}}, \tag{17}$$

where $k_{1,\text{gb}} = 113\,\text{kg}\,\text{kN}^{-1}\,\text{m}^{-1}$, $b_{\text{gb}} = 0.71$, $p_{2,\text{gb}} = 12.9$ € kg^{-1} and τ is the peak input torque to the gearbox in kNm.

OpEx (gStation.gearbox.opex)

Not modelled due to lack of information and data.

4.2.2 Generator (gStation.gen)

The electrical generator cost for GG AWESs is modelled here. For FG, the generator cost is under the kite cost model (section 2). The cost of the generator depends on the torque as well as speed. High torque requires stronger and robust components within the generator whereas high speed requires high precision, wear resistance etc. Due to unavailability of detailed data, here we have modelled the cost as a function of power.

CapEx approach 1 (gStation.gen.one.capex)

The cost of the generator is modelled as

$$C_{\text{gen}} = p_{1,\text{gen}} P_{\text{rated,gen}}, \tag{18}$$

where $p_{1,\text{gen}} = 120$ € kW^{-1} and $P_{\text{rated,gen}}$ is the electrical rated power of the generator.

The generator rating will be driven by the peak mechanical power during reel-out. As a probable ballpark value, this peak mechanical reel-out power could be 2.5 times the electrical rated power.

CapEx approach 2 (gStation.gen.two.capex)

Generator costs can be modelled similarly to that modelled for conventional wind turbines. The wind turbine-rated power is analogous to the maximum electrical reel-out power for GG AWES. The cost functions used in the WISDEM tool by NREL [10] are as follows:

$$m_{\text{gen}} = k_{\text{gen}} P_{\text{rated,gen}} + b_{\text{gen}}, \tag{19}$$

$$C_{\text{gen}} = p_{2,\text{gen}} m_{\text{gen}}, \tag{20}$$

where $k_{\text{gen}} = 2.3\,\text{kg}\,\text{kW}^{-1}$, $P_{\text{gen,rated}}$ is the electrical rated power of the generator in kW, $b_{\text{gen}} = 3400$, and $p_{2,\text{gen}} = 12.4$ € kg^{-1}. The generator capacity will be driven by the peak mechanical power during reel-out.

OpEx

Not modelled due to lack of information and data.

4.2.3 Electrical storage (gStation.elecSto)

The objective of storage is to act as an intermediate energy exchanger to charge and discharge during cycle operation to maintain the average cycle power at the grid side. The amount of storage required will be driven by the energy exchange required for this purpose. This is explained in [24].

The electrical storage solution could either be an ultracapacitor bank or a battery bank. The ultracapacitor bank and the battery bank have different requirements for sizing and have different cost and lifetime specifications. The ultracapacitors can withstand high C-rates (charge-discharge rates) of 100C or more. Whereas, the batteries typically have a low C-rate of around 0.5-1C. This drives the sizing of the two options. A 1C rate means that the discharge current will discharge the entire battery in 1 hour.

Ultracapacitor bank (elecSto_type=1)

An ultracapacitor bank is a high-capacity energy storage system composed of multiple ultracapacitor modules connected in parallel or series. Unlike traditional batteries, ultracapacitors store energy electrostatically, enabling rapid charge and discharge cycles with high efficiency. They are commonly used in applications requiring burst power delivery, energy recuperation, fast charging capabilities, and tolerance to frequent cycling.

CapEx (gStation.elecSto.ultracap.capex)

The costs are modelled as

$$C_{\text{elecSto,uc}} = p_{\text{elecSto,uc}} E_{\text{rated,elecSto,uc}}. \tag{21}$$

where $p_{\text{elecSto,uc}} = 60{,}000$ €/kWh and $E_{\text{rated,elecSto}}$ is the required storage sizing in kW h. This is driven by the maximum energy exchanged by the ultracapacitor during the cycle operations for all the wind speeds in the operational range.

In absence of detailed power generation profile inputs for GG systems, assuming a 60 s cycle time, out of which 40 s is the reel-out time, negligible reel-in power requirement, this energy can be approximated in kW h as

$$E_{\text{rated,elecSto,uc}} = P_{\text{rated,AWES}} \frac{20}{3600}, \tag{22}$$

where $P_{\text{rated,AWES}}$ is in kW.

For FG systems, the energy stored by the ultracapacitor in kW h is equal to half of the potential energy swept over a loop

$$E_{\text{rated,elecSto,uc}} = mgR_0 \frac{1}{3.6 \cdot 10^6}, \tag{23}$$

where m is the AWES mass, $g = 9.81$ m/s^2 is the gravitational acceleration and R_0 is the maximum turning radius, which approximates the height difference between the top part of the loop and the bottom. If no detailed information are available, it can be assumed $R_0 = 5b$, where b is the wingspan.

It should be checked that the sizing of ultracapacitors is within the usual C-rating of around 100 C.

OpEx (gStation.elecSto.ultracap.opex)

Due to a large number of charging and discharging cycles during operation, the lifetime of the ultracapacitors is driven by the maximum number of charge-discharge cycles $N_{\text{elecSto,uc}}$ indicated by the manufacturer (typically around $N_{\text{elecSto,uc}} = 10^6$). This lifetime can be calculated based on the charge-discharge cycles for the specific AWES based on its operational behaviour in the given wind speed probability distribution as follows:

$$N_{\text{cycles,elecSto,uc}} = \left(8760 \int_{v_{\text{in}}}^{v_{\text{out}}} f(v_{\text{w}}) \frac{E_{\text{ex,elecSto,uc}}(v_{\text{w}})}{\Delta t_{\text{cycle}}(v_{\text{w}})} \text{d}v_{\text{w}} \right) / E_{\text{rated,elecSto,uc}}, \tag{24}$$

where $N_{\text{cycles,elecSto,uc}}$ is the number of charge-discharge cycles in one year, v_{in} is the cut-in wind speed, v_{out} is the cut-out wind speed, $f(v_{\text{w}})$ is the wind speed probability distribution, $E_{\text{ex,elecSto,uc}}(v_{\text{w}})$ is the energy exchanged by the ultracapacitor bank every cycle in kWh, $\Delta t_{\text{cycle}}(v_{\text{w}})$ is the cycle time in h, and $E_{\text{rated,elecSto,uc}}$ is the energy rating of the capacitor in kWh.

The frequency of replacement of the ultracapacitor bank is

$$f_{\text{repl,elecSto,uc}} = \frac{N_{\text{cycles,elecSto,uc}}}{N_{\text{elecSto,uc}}}. \tag{25}$$

In absence of detailed inputs, $N_{\text{cycles,elecSto,uc}}$ can be approximated for GG systems by considering

$$\frac{E_{\text{ex,elecSto,uc}}(v_{\text{w}})}{\Delta t_{\text{cycle}}(v_{\text{w}})} = \frac{E_{\text{rated,elecSto,uc}}/2}{60/3600} = 30 E_{\text{rated,elecSto,uc}}, \tag{26}$$

using the same assumptions as used in the CapEx section. The amount of energy exchanged increases with increasing wind speed and is maximum at rated wind speed, after which it remains constant [24]. Therefore, as an approximation, $E_{\text{ex,elecSto,uc}}(v_{\text{w}})$ is approximated to half of the maximum value for all wind speeds. The number of cycles in one year can be then approximated with $N_{\text{cycles,elecSto,uc}} \approx 250,000$.

For FG systems, the amount of energy exchanged can be assumed constant as function of wind speed, so that the number of $N_{\text{cycles,elecSto,uc}}$ is the actual number of loops. $N_{\text{cycles,elecSto,uc}}$ can be estimated by modelling the loop period as

$$\Delta t_{\text{cycle}} \approx \frac{2\pi R_0(v_{\text{w}})}{\lambda(v_{\text{w}}) v_{\text{w}}}, \tag{27}$$

where R_0 is the turning radius and λ is the the wing speed to wind speed ratio. Therefore for FG AWESs, Eq. (24) can be then simplified to

$$N_{\text{cycles,elecSto,uc}} = 8760 \int_{v_{\text{in}}}^{v_{\text{out}}} f(v_{\text{w}}) \frac{\lambda(v_{\text{w}}) v_{\text{w}}}{2\pi R_0(v_{\text{w}})} \text{d}v_{\text{w}}, \tag{28}$$

where, if no detailed information are available, the wing speed ratio and the turning radius can be assumed to be independent of the wind speed as $\lambda = 7$ and $R_0 = 5b$.

Battery bank (elecSto_type=2)

A typical Li-ion battery bank is a high-capacity energy storage system composed of multiple battery cells or modules connected in parallel or series. Unlike ultracapacitors, batteries store energy chemically, providing a more consistent and prolonged power supply. Battery banks are widely used in applications such as in renewable energy systems, uninterruptible power supplies (UPS), electric vehicles, and grid energy storage.

CapEx (gStation.elecSto.batt.capex)

To use the battery banks for power smoothing, they need to be sized such that the charging or discharging does not exceed 1 C. In absence of detailed power generation profile inputs, assuming negligible reel-in power requirement and considering 1 C rating, this energy can be approximated in kW h as

$$E_{\mathrm{rated,elecSto,batt}} = P_{\mathrm{rated,AWES}}, \tag{29}$$

where $P_{\mathrm{rated,AWES}}$ is in kW

The costs are modelled the same as ultracapacitors with $p_{\mathrm{elecSto,batt}} = 200$ €/kWh.

OpEx (gStation.elecSto.batt.opex)

The costs are modelled the same as that of ultracapacitors with $N_{\mathrm{elecSto,batt}} = 10^4$.

4.2.4 Power converter (gStation.powerConv)

Power converters are electronic devices that transform electrical energy from one form to another, commonly alternating current (AC) to direct current (DC) or vice versa. They regulate the voltage, frequency, and waveform to match the requirements of various electrical systems, facilitating efficient energy transfer.

CapEx (gStation.powerConv.capex)

The two power converters in this drivetrain will be sized differently. The converter connected to the generator will be sized for the generator power rating, whereas the converter at the grid side will be sized by the rated power of the AWES.

The cost of the power converters is modelled as

$$C_{\mathrm{pc}} = p_{\mathrm{pc}} P_{\mathrm{rated,pc}}. \tag{30}$$

where p_{pc} is 100 € kW^{-1} and $P_{\mathrm{rated,pc}}$ is the input electrical power to the converter.

OpEx (gStation.powerConv.opex)

Not modelled due to lack of information and data.

4.3 Hydraulic drivetrain (drivetrain_type=2)

This drivetrain concept is more suitable for GG systems. Primary components of this concept are shown in fig. 8 and is described in [27, 24, 28]. The winch drives a pump-motor machine which is connected to a hydropneumatic accumulator bank and a hydraulic motor which drives the generator. A hydro-pneumatic accumulator is a vessel capable of storing energy in the form of a compressed gas.

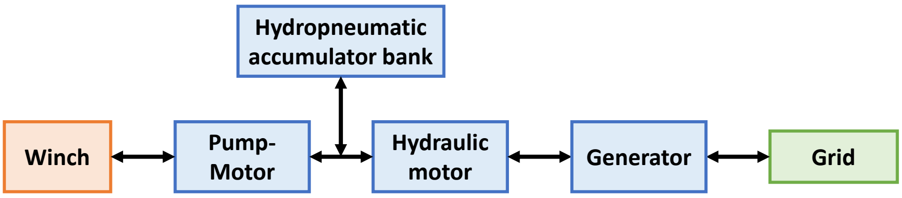

Figure 8: Hydraulic drivetrain architecture (adapted from [24]).

4.3.1 Pump-Motor (gStation.pumpMotor)

Pump-motor machines refer to systems where a pump and a motor are combined into a single unit. This unit can either be driven as a pump using a mechanical input, such as the winch rotation, or can be driven as a motor using an hydraulic input, such as from a hydropneumatic accumulator bank.

CapEx (gStation.pumpMotor.capex)

The CapEx of the pump-motor machine is modelled as

$$C_{\mathrm{pm}} = p_{1,\mathrm{pm}} P_{\mathrm{rated,pm}}, \tag{31}$$

where $p_{1,\mathrm{pm}} = 100$ € kW^{-1} and $P_{\mathrm{rated,pm}}$ is the rated power of the machine which is driven by the peak mechanical power during reel-out.

OpEx (gStation.pumpMotor.opex)

Depending on operating conditions (e.g. effective capacity factor, wind speed variations), a major maintenance of 2-4 times during the life is expected. This should typically decrease with product maturity.

$$OM_{\mathrm{pm}} = f_{\mathrm{om,pm}} p_{2,\mathrm{pm}} P_{\mathrm{rated,pm}}, \tag{32}$$

where $f_{\mathrm{om,pm}} = 1/8$ year^{-1} and $p_{2,\mathrm{pm}} = 75$ € kW^{-1}.

4.3.2 Hydropneumatic accumulator bank (gStation.hydAccum)

The hydropneumatic accumulator has two chambers divided by a separator. The first chamber is a fluid chamber, usually filled with hydraulic oil, and the second is a gas chamber, usually containing nitrogen. The fluid chamber is connected to the hydraulic circuit. The winch drives the pump-motor machine in the reel-out phase which pumps the hydraulic fluid in the accumulator bank under high pressure. This accumulator bank is charged and discharged during the cycle to maintain a smooth power output at the grid side.

CapEx (gStation.hydAccum.capex)

The cost of the hydropneumatic accumulator bank can be modelled as

$$C_{\mathrm{hacc}} = p_{1,\mathrm{hacc}} E_{\mathrm{rated,hacc}}, \tag{33}$$

where $p_{1,\mathrm{hacc}} = 30{,}000$ € kW^{-1} h^{-1} and $E_{\mathrm{rated,hacc}}$ is the required storage sizing in kW h. This is driven by maximum energy exchanged by the accumulator bank during the cycle operations for all the wind speeds in the operational range. The calculation of $E_{\mathrm{rated,hacc}}$ is similar to $E_{\mathrm{rated,uc}}$, as mentioned in the Ultracapacitor bank section

OpEx (gStation.hydAccum.opex)

The maintenance cost of the hydropneumatic accumulator bank can be modelled as

$$OM_{\text{hacc}} = f_{\text{om,hacc}} p_{2,\text{hacc}} E_{\text{rated,hacc}}, \tag{34}$$

where $f_{\text{on,hacc}} = 1/10\ \text{year}^{-1}$ and $p_{2,\text{hacc}} = 1200$ € $\text{kW}^{-1}\,\text{h}^{-1}$.

4.3.3 Hydraulic motor (gStation.hydMotor)

Hydraulic motors are machines that convert hydraulic energy (the pressure and flow of hydraulic fluid) into mechanical energy (rotary motion). They are commonly used in hydraulic systems where the power source is a hydraulic pump. This unit is integrated with a controller and is used to drive the generator.

CapEx (gStation.hydMotor.capex)

The CapEx of the hydraulic motor machine is modelled as

$$C_{\text{hm}} = p_{1,\text{hm}} P_{\text{rated,hm}}, \tag{35}$$

where $p_{1,\text{hm}} = 200$ € kW^{-1} and $P_{\text{rated,hm}}$ is driven by the rated power of the AWES.

OpEx (gStation.hydMotor.opex)

The maintenance of the hydraulic motor machine is modelled as

$$OM_{\text{hm}} = f_{\text{om,hm}} p_{2,\text{hm}} P_{\text{rated,hm}}, \tag{36}$$

where $f_{\text{om,hm}} = 1/12\ \text{year}^{-1}$ and $p_{2,\text{hm}} = 80$ € kW^{-1}.

4.3.4 Generator (gStation.gen)

The generator rating will be driven by the rated power of the AWES. The cost model is the same as described in section 4.2.2.

4.4 Launch & land system (gStation.lls)

The launch and land system (LLS) performs the launch of the kite into the air and its controlled descent for landing. The LLS would be different for different AWE concepts. There are two commonly used approaches: 1) Horizontal take-off and landing (HTOL), which either uses a catapult or a rotatory accelerated platform; and 2) Vertical take-off and landing (VTOL), which uses electric propellers. On one hand, HTOL has much larger spatial requirements than VTOL and this significantly drives up the cost of the supporting infrastructure, but on the other hand VTOL significantly drives up the kite's structural mass and consequently the cost. VTOL is most certainly the preferred design choice for FG systems.

These costs are not modelled due to lack of information and data.

4.5 Yaw system (gStation.yaw)

A yaw system is a mechanism that controls the orientation of the winch and the drivetrain relative to the wind direction. It allows the system to optimize power generation by adjusting their alignment to capture maximum incoming wind. Yaw systems typically incorporate sensors, actuators, and control algorithms to continuously monitor wind direction and adjust the orientation accordingly.

These costs are expected to scale with the mass of the ground station. But, they are not modelled due to lack of information and data.

4.6 Control station (gStation.controlStation)

The control station facilitates real-time data exchange between the kite and the ground station, ensuring optimal and safe operation of the system throughout its flight.

These costs are not modelled due to lack of information and data.

5 Balance of system (BoS)

Balance of System (BoS) components are defined as all components except the primary system components (i.e. except the kite, tether, and ground station) for a single AWES. These costs are more relevant for the evaluations of specific business cases.

These costs will be highly dependent on the type and size of the AWES and as well as on the site-specific considerations. These considerations can cause order of magnitude changes in the results for different scenarios. The cost references proposed in this section are under the assumption of an onshore installation and the uncertainty is relatively higher than earlier sections.

5.1 Site preparation (BoS.sitePrep)

Costs under site preparation could include removing obstacles such as vegetation, debris, and uneven terrain that could interfere with the launch, flight, or landing of the kite. Additionally, any necessary groundwork such as levelling the surface or installing protective barriers may be undertaken to optimise the site for efficient and uninterrupted operation of the system. These costs are modelled as

$$C_{\mathrm{sitePrep}} = p_{\mathrm{sitePrep}} P_{\mathrm{rated}}, \tag{37}$$

where $p_{\mathrm{sitePrep}} = 40$ € kW^{-1} and P_{rated} is the rated electrical power of the AWES.

5.2 Foundation & Support structure (BoS.found)

Foundations and support structures are designed to withstand the forces generated by the AWES during operation and support the ground station weight. These foundations can vary in design depending on factors like soil conditions, site location, and system requirements. The launch and land apparatus is also an important cost driver for this component. Moreover, these costs will be significantly different for onshore, offshore bottom-fixed and offshore floating scenarios. These costs are modelled as

$$C_{\mathrm{found}} = p_{\mathrm{found}} P_{\mathrm{peak}}, \tag{38}$$

where $p_{\mathrm{found}} = 55$ € kW^{-1} and P_{peak} is the peak power generated by the AWES.

5.3 Installation & Commissioning (BoS.install)

Installation and commissioning involves assembling and configuring components to ensure proper functionality and performance. This process includes erecting support structures, connecting power and communication systems, and testing operational parameters. In addition, commissioning involves fine-tuning control algorithms, conducting safety checks, and verifying compliance with regulatory standards. These costs are modelled as

$$C_{\mathrm{install}} = p_{\mathrm{install}} P_{\mathrm{rated}}, \tag{39}$$

where $p_{\mathrm{install}} = 40$ € kW^{-1} and P_{rated} is the rated electrical power of the AWES.

5.4 Operations & Maintenance (BoS.OM)

These costs include all the yearly costs necessary for the operation and maintenance of the BoS. It could include, for example, the lease of the land used and the insurance costs against potential risks and liabilities associated with their deployment and operation. These costs are modelled as

$$OM_{\mathrm{BoS}} = p_{\mathrm{BoS,OM}} P_{\mathrm{rated}} \tag{40}$$

where $p_{\mathrm{BoS,OM}} = 60$ € kW^{-1} per year and P_{rated} is the rated electrical power of the AWES.

5.5 Decommissioning (BoS.decomm)

Decommissioning entails the safe dismantling and removal of components at the end of their operational lifespan or in case of system retirement. This process involves disassembling support structures, disconnecting power and communication systems, and responsibly disposing of materials in accordance with environmental regulations. These costs are modelled as

$$C_{\text{decomm}} = f_{\text{install}} C_{\text{install}}, \tag{41}$$

where $f_{\text{install}} = 0.5$ and C_{install} are the Installation & Commissioning costs.

6 Balance of plant (BoP)

Balance of Plant (BoP) components are defined as all components of an AWE wind farm (flock), except the individual systems themselves. These costs will be relevant for the evaluation of specific business cases, and for the design of the flock layout.

These costs are not modelled due to the lack of information and data.

6.1 Array cables (BoP.arrayCables)

Array cables, also known as inter-array cables, connect individual AWESs within an AWE flock to a central point, typically a substation. These cables transmit the electricity generated by the individual systems to the point of collection, where it is then transferred to the onshore grid or distributed further. The cost of these cables is a function of the distance between the systems, and hence they will play a significant role in driving the layout of an AWE flock.

6.2 Substations (BoP.substations)

Substations serve as central hubs for collecting and transforming electricity generated by AWES in a flock. They typically house transformers to adjust voltage levels for transmission and may include other power electronics to regulate the power flow.

6.3 Grid integration (BoP.gridInt)

Grid integration involves the connection of the AWE flock to the existing power grid infrastructure. This includes the costs of the power electronics required to synchronise with the voltage and frequency of the grid and compliance with regulatory standards. This could also include the costs of the export cables from the substation to the point of connection to the grid.

7 Design metrics (metrics)

Design metrics are quantitative measures used to evaluate the performance, efficiency, and effectiveness of a system or product during the design process. These metrics can be used as objectives in design optimisation frameworks. Following are the key identified design metrics.

7.1 Levelized cost of energy (metrics.LCOE)

The most commonly used design metric in the industry is the levelized cost of electricity (LCoE) which can be calculated as shown in the following equation:

$$\mathrm{LCoE} = \frac{\sum_{y=0}^{N_\mathrm{y}} \frac{\mathrm{CapEx_y} + \mathrm{OpEx_y}}{(1+r)^y}}{\sum_{y=0}^{N_\mathrm{y}} \frac{\mathrm{AEP_y}}{(1+r)^y}}, \tag{42}$$

where CapEx is the capital expenditure, OpEx is the operational expenditure, r is the discount rate, AEP is the annual energy produced, y is the instantaneous year, and N_y is the project lifetime.

The final discount rate is usually a result of the different discount rates for equity and debt components weighted according to their proportions in total financing. This is also known as the weighted average cost of capital (WACC). If a project is financed with a debt to equity ratio of 'q', then the WACC, or the final discount rate

$$r = \frac{q}{1+q} r_\mathrm{d}(1 - T_\mathrm{C}) + \frac{1}{1+q} r_\mathrm{e}, \tag{43}$$

where r_d is the cost of debt, r_e is the cost of equity, T_C is the tax rate for corporations. Typical values for wind energy projects are $q = 70/30$, $r_\mathrm{d} = 0.08$, $r_\mathrm{e} = 0.12$, and $T_\mathrm{C} = 0.25$.

The wind industry is slowly evolving to explore design metrics beyond LCoE. Following subsections discuss the key literature proposing such metrics.

7.2 Levelized profit of energy (metrics.LPoE)

The levelized profit of energy (LPoE) captures the influence of the dynamic nature of the EU day-ahead electricity market [20]. It is essentially the difference between levelized revenue of electricity (LRoE) and LCoE as shown below

$$\mathrm{LPoE} = \mathrm{LRoE} - \mathrm{LCoE}, \tag{44}$$

where

$$\mathrm{LRoE} = \frac{\sum_{y=0}^{N_\mathrm{y}} \frac{(p_\mathrm{y} + \mathrm{subsidy_y})\mathrm{AEP_y}}{(1+r)^y}}{\sum_{y=0}^{N_\mathrm{y}} \frac{\mathrm{AEP_y}}{(1+r)^y}}, \tag{45}$$

where $\mathrm{subsidy_y}$ is the amount of subsidy received in year y, r is the discount rate and p_y is the mean electricity price as seen by the AWE unit in year y, given by

$$p_\mathrm{y} = \left(8760 \int_{v_\mathrm{in}}^{v_\mathrm{out}} f(v_\mathrm{w}) p(v_\mathrm{w}) P(v_\mathrm{w}) \mathrm{d}v_\mathrm{w} \right) / \mathrm{AEP_y}. \tag{46}$$

For reference, a subsidy of 50€ $\mathrm{MW^{-1}\,h^{-1}}$ could be assumed.

The energy price p can be modelled as a function of wind speed v_w using a a linear model based on historic data:

$$p(v_\mathrm{w}) = p_0 + p_1 v_\mathrm{w}. \tag{47}$$

Two examples from Germany evaluated in [20] are given in Table 7.

Table 7: Electricity price parameters [20]

	p_0 [€/MWh]	p_1 [(€/MWh)/(m/s)]
Onshore	45	-1.2
Offshore	45	-0.9

7.3 Cost of Valued Energy (metrics.CoVE)

The Cost of Valued Energy CoVE [18] informs about the ratio of costs to revenue. CoVE is similar to LCOE, with the difference that CoVE is weighting (valuing) energy based on the spot market price. In particular, CoVE takes the same value of LCOE with the energy prices are constant. It is defined as

$$\mathrm{CoVE} = \frac{\sum_{y=0}^{N_\mathrm{y}} \frac{\mathrm{CapEx_y}+\mathrm{OpEx_y}}{(1+r)^y}}{\sum_{y=0}^{N_\mathrm{y}} \frac{\mathrm{vf_y}\,\mathrm{AEP_y}}{(1+r)^y}}, \tag{48}$$

where the value factor $\mathrm{vf_y}$ is ratio between the mean electricity price as seen by the AWE unit p_y (Eq. 46) and the mean electricity price of the grid $\hat{p}$ [17],

$$\mathrm{vf_y} = \frac{p_\mathrm{y}}{\hat{p}}, \tag{49}$$

where $\hat{p}$ is the electricity average price of the grid

$$\hat{p} = \int_0^{+\infty} f(v_\mathrm{w})p(v_\mathrm{w})\mathrm{d}v_\mathrm{w}. \tag{50}$$

Producing when the energy price is high is then increasing the CoVE.

7.4 Net present value (metrics.NPV)

The Net present value (NPV) is the discounted value to the cash flow over the lifetime. It is calculated as

$$\mathrm{NPV} = \sum_{y=0}^{N_\mathrm{y}} \frac{(p_\mathrm{y} + \mathrm{subsidy_y})\mathrm{AEP_y} - \mathrm{CapEx_y} - \mathrm{OpEx_y}}{(1+r)^y}, \tag{51}$$

where the definitions of parameters is retained from earlier sections.

7.5 Internal rate of return (metrics.IRR)

The internal rate of return (IRR) is used to estimate the profitability of potential investments. IRR is a discount rate that makes the net present value (NPV) equal to zero. Therefore it can be calculated by solving for r in Equation (51) such that NPV = 0.

7.6 Levelised impact of energy (metrics.LIoE)

The Levelized impact of energy (LIoE) is a metric used to evaluate the environmental impact of energy generation over the entire lifetime [19]. It can consider factors such as carbon emissions, air and water pollution, land use, resource depletion, etc. The calculation of LIoE involves assessing the total impact of energy production and distribution, including all stages from extraction or generation to end use and disposal or decommissioning. It is defined as

$$\mathrm{LIoE} = \frac{\sum_{y=0}^{N_\mathrm{y}} \frac{Q_\mathrm{y}}{(1+r)^y}}{\sum_{y=0}^{N_\mathrm{y}} \frac{\mathrm{AEP}_\mathrm{y}}{(1+r)^y}}, \tag{52}$$

where Q_y is the CO_2-equivalent green house gas (GHG) emissions of the AWES during year y, and the the definitions of other parameters is retained from earlier sections.

A life cycle analysis (LCA) model is needed to compute Q_y. This can be build from LCA studies such as [29].

8 Potential markets

This section describes some of the potential markets to deploy airborne wind energy systems.

8.1 Project specific parameters

Some common project specific business case parameters include the project lifetime, number of units, wind resource, and market-related parameters like the discount rate, revenue generation scheme etc. Following are some of the parameters that should be modelled with detail.

8.1.1 Wind resource

The wind resources are assumed to be evaluated at a reference height h_{ref}. The wind speed varies as a function of height given by

$$v_{\mathrm{w}}(h) = v_{\mathrm{w}}(h_{\mathrm{ref}}) \left(\frac{h}{h_{\mathrm{ref}}}\right)^{\alpha}, \tag{53}$$

where v_{w} is wind speed, h is height, and α is the wind shear coefficient.

The wind distribution at h_{ref} is modelled using Weibull distribution as

$$f(v_{\mathrm{w}}, h_{\mathrm{ref}}) = \frac{k}{A} \left(\frac{v_{\mathrm{w}}}{A}\right)^{k-1} e^{-(v_{\mathrm{w}}/A)^{k}}, \tag{54}$$

where k is the shape parameter and A is the scale parameter for a given location. The scale parameter can be expressed in terms of mean wind speed for a particular site using

$$A = \frac{v_{\mathrm{w,mean}}}{\Gamma(1+\frac{1}{k})}. \tag{55}$$

where Γ is the Gamma function (generally a built-in function in programming languages).

8.1.2 Learning and scaling factors

The use of learning factors in projecting costs of AWESs is described in [20]. Different terminologies for learning factors have been used in the literature depending on the field of study. Experience and learning are generally used for cumulative production, and scale is used for size. If the cumulative production capacity or size is doubled, the specific costs reduce by a factor of 2^b. The learning rate is defined as $1 - 2^b$, and b is called the learning elasticity.

The model should account for scale-up benefits in terms of cost per kW of installed power. This considers the effects such as make–buy optimisation, reducing relative manpower costs, technological advancements, and others. To take these benefits into account, two learning elasticities are introduced: a for scale (size) and b for experience (cumulative production). The learning factors can be applied as follows:

$$C = C_0 \left(\frac{S}{S_0}\right)^{a} \left(\frac{Q}{Q_0}\right)^{b} \tag{56}$$

where C is the scenario unit cost, C_0 is the reference unit cost, S is the scenario size, S_0 is the reference size, Q are the scenario units, and Q_0 are the reference units. The learning elasticities can also be used per subsystem based on the known data points from literature belonging to the relevant industries, such as conventional wind turbines, aviation, solar PV (for BoS and BoP), etc.

Costs parameters can vary largely according to the industrialisation level of the production. The recognised levels of production are listed in table 8.

Table 8: Different types of production scales.

Production	Description
Prototype	2 - 5 test units/pilots
Series	Batch-wise production capability with early impacts of economies of scale (e.g., 50+ units)
Mass	Continuous production capability with matured impacts of economies of scale (e.g., 1000+ units)

8.2 Grid connected

This market corresponds to having either a single unit or a flock (multiple AWESs) connected to the public electricity grid of a country. This is aligned with the market of grid-connected wind farms developed by utility companies through the tendering process of different countries.

For system design and optimisation studies, a case of a single system connected to the grid can be evaluated by only including the Balance of System (section 5) costs, and excluding the Balance of Plant (section 6) costs.

This market can be further categorised into:

8.2.1 Onshore

In the onshore setting, AWESs would typically be situated on grass lands or farm lands away from residential areas. It could also include regions with complex terrains. These installations are characterised by their accessibility and relatively lower installation costs compared to the offshore counterparts.

For a typical on-shore case in Europe, the following wind resources parameters can be considered as a reference [14]: $h_{\mathrm{ref}} = 100$ m, α=0.14, $A = 8$ m/s and k = 2.

8.2.2 Offshore

Offshore AWESs could be deployed in bodies of water, such as seas or oceans, providing significant advantages in terms of wind consistency and availability. While offshore installations involve higher upfront costs and more complex logistics, they offer immense potential for energy generation without any impact on land use.

For a typical off-shore case in the North sea, the following wind resources parameters can be considered as a reference [14]: $h_{\mathrm{ref}} = 100$ m, α=0.1, $A = 9.5$ m/s and k = 2.1.

8.3 Off-grid hybrid power systems

In contrast to grid-connected systems, the off-grid scenario entails the operation of AWES independently from the public electricity grid. These systems are often deployed in remote or off-grid locations where grid connection is impractical or unavailable and the majority of the electricity demand is supplied by using Diesel generators. These areas usually have expensive logistics due to lesser accessibility and infrastructure. Off-grid setups require integrated energy storage solutions and localized distribution infrastructure to provide reliable power supply to isolated communities or facilities. An off-grid hybrid power system is defined as an independent but locally coupled power system using combinations of AWE, Solar PV, Diesel generators and Batteries [30].

For a typical off-grid case, the following wind resources parameters can be considered as a reference: $h_{\mathrm{ref}} = 100$ m, α=0.14, $A = 8$ m/s and k = 2.

8.4 Temporary installations

Temporary deployments of AWESs may be utilized for a range of objectives, including disaster relief, auxiliary power provision, or addressing temporary energy requirements in isolated areas. This drives requirements such as swift deployment, flexibility and adaptability from the systems.

8.5 Power-to-X

The Power-to-X concept involves the conversion of electricity into other forms of energy or products. This includes processes such as electrolysis to produce hydrogen (Power-to-Hydrogen), synthesis of synthetic fuels (Power-to-Fuels), or production of other valuable commodities like chemicals or heat. Power-to-X technologies play a crucial role in energy storage, grid balancing, and decarbonization efforts, enabling the utilization of renewable energy in various sectors beyond electricity generation.

Nomenclature

Parameters

A	Weibull scale parameter
α	Wind shear exponent
$\mathcal{R}$	Wing aspect ratio
b	Wing span
d	Diameter
E	Energy
F	Force
Γ	Gamma function
g	Gravity
h	Height
k	Weibull shape parameter
λ	Wing speed to wind speed ratio
L	Component lifetime
l	Length
m	Mass
N	Number
P	Power
p	Price
q	Debt-to-equity ratio
ρ	Density
r	Discount rate
σ	Strength
S	Projected wing area
τ	Torque
t	Thickness
v	Velocity

Subscripts

al	Aluminium
arrayCables	Array cables
At	Factor area tether
avio	Avionics
batt	Batteries
batt	Battery bank
coat	Coating
cs	Control station
decomm	Decommissioning
elecSto	Electrical storage
found	Foundation and support structure
gb	Gearbox
gen	Generator
gridInt	Grid integration

gStation Ground station
hacc Hydro-pnuematic accumulator
hm Hydraulic motor
hydAccum Hydro-pnuematic accumulator
hydMotor Hydraulic motor
in Cut-in
install Installation & Commissioning
lls Launch & land system
maint Maintenance
mat Material
ob Onboard
OM Operation & Maintenance
out Cut-out
pc Power converter
pm Pump-Motor machine
powerConv Power converter
prop Propulsion
ref Reference
repl Replacement
sitePrep Site preparation
str Structure
st Steel
tAttach Tether attachment
t Tether
uc Ultracapacitor bank
wet Wetted surface
winch Winch
w Wind
yaw Yaw system
y Year

Acronyms

AEP Annual energy production
AWES Airborne wind energy system
BoP Balance of plant
BoS Balance of system
CapEx Captial expenditure
CoVE Cost of valued energy
CRL Commercial readiness level
FG Fly-generation
GG Ground-generation
IRR Internal rate of return
LCA Life cycle analysis
LCoE Levelized cost of energy
LF Loading factor

LIoE	Levelized impact of energy
LPoE	Levelized profit of energy
NPV	Net present value
OpEx	Operational expenditure
SF	Safety factor
TRL	Technology readiness level
WACC	Weighted average cost of capital

References

[1] *Airborne Wind Europe*. (accessed on April 14, 2023). 2023. URL: https://airbornewindeurope.org/.

[2] *Reference Economic Model for Airborne Wind Energy Systems*. (accessed on April 24, 2024). URL: https://github.com/awegroup/AWE-Eco.

[3] *IEA Wind Task 48 on Airborne Wind Energy*. (accessed on April 14, 2023). 2021. URL: https://iea-wind.org/task48/.

[4] Jannis Heilmann and Corey Houle. "Economics of Pumping Kite Generators". In: *Airborne Wind Energy. Green Energy and Technology. Springer Berlin Heidelberg*. Ed. by Uwe Ahrens, Moritz Diehl, and Roland Schmehl. 2013, pp. 271–284. DOI: 10.1007/978-3-642-39965-7_15.

[5] Christoph Grete. "Optimization, Scaling and Economics of Pumping Kite Power Systems, MSc thesis, Delft University of Technology". In: (2014). URL: http://resolver.tudelft.nl/uuid:b980aab7-f346-4030-97a3-a3cde13a51d6.

[6] M. De Lellis, A. K. Mendonça, R. Saraiva, A. Trofino, and Lezana. "Electric power generation in wind farms with pumping kites: An economical analysis". In: *Renewable Energy* 86 (2016), pp. 163–172. DOI: 10.1016/j.renene.2015.08.002.

[7] Pietro Faggiani and Roland Schmehl. "Design and Economics of a Pumping Kite Wind Park". In: *Airborne Wind Energy. Green Energy and Technology. Springer, Singapore*. Ed. by Roland Schmehl. 2018, pp. 391–411. DOI: 10.1007/978-981-10-1947-0_16.

[8] Florian Bauer, Ralph M. Kennel, Christoph M. Hackl, Filippo Campagnolo, Michael Patt, and Roland Schmehl. "Drag power kite with very high lift coefficient". In: *Renewable Energy* 118 (2018), pp. 290–305. ISSN: 18790682. DOI: 10.1016/j.renene.2017.10.073.

[9] BVG Associates. *Wind farm costs – Guide to an offshore wind farm*. (Accessed on 03/20/2023). Jan. 2019. URL: https://guidetoanoffshorewindfarm.com/wind-farm-costs.

[10] NREL. *Theory — WISDEM 2.0 documentation on cost scaling*. (Accessed on 03/20/2023). URL: https://wisdem.readthedocs.io/en/master/wisdem/nrelcsm/theory.html.

[11] Mario Garcia-Sanz. "A Metric Space with LCOE Isolines for Research Guidance in wind and hydrokinetic energy systems". In: *Wind Energy* 23.2 (2020), pp. 291–311. DOI: https://doi.org/10.1002/we.2429. eprint: https://onlinelibrary.wiley.com/doi/pdf/10.1002/we.2429. URL: https://onlinelibrary.wiley.com/doi/abs/10.1002/we.2429.

[12] Nicholas Tucker. "Airborne Wind Turbine Performance: Key Lessons From More Than a Decade of Flying Kites." In: *The Energy Kite Part I*. Ed. by P. Echeverri, T. Fricke, G. Homsy, and N. Tucker. 2020, pp. 93–224. URL: https://x.company/projects/makani/#.

[13] Filippo Trevisi, Mac Gaunaa, and Michael McWilliam. "Unified engineering models for the performance and cost of Ground-Gen and Fly-Gen crosswind Airborne Wind Energy Systems". In: *Renewable Energy* 162 (2020), pp. 893–907. DOI: 10.1016/j.renene.2020.07.129.

[14] Tyler Stehly, Philipp Beiter, and Patrick Duffy. *2019 Cost of Wind Energy Review.* Tech. rep. NREL/TP-5000-78471. National Renewable Energy Laboratory, 2020. URL: https://www.nrel.gov/docs/fy21osti/78471.pdf.

[15] *Getting airborne – the need to realise the benefits of airborne wind energy for net zero.* Tech. rep. BVG Associates on behalf of Airborne Wind Europe, Sept. 2022. URL: https://airbornewindeurope.org/wp-content/uploads/2023/03/BVGA-Getting-Airborne-White-Paper-220929.pdf.

[16] Vignesh Ramasamy, Jarett Zuboy, Eric O'Shaughnessy, David Feldman, Jal Desai, Michael Woodhouse, Paul Basore, and Robert Margolis1. *U.S. Solar Photovoltaic System and Energy Storage Cost Benchmarks, With Minimum Sustainable Price Analysis: Q1 2022.* Tech. rep. National Renewable Energy Laboratory, 2022. URL: https://www.nrel.gov/docs/fy22osti/83586.pdf.

[17] Lion Hirth and Simon Müller. "System-friendly wind power. How advanced wind turbine design can increase the economic value of electricity generated through wind power". In: *Energy Economics* 56 (2016), pp. 51–63. ISSN: 01409883. DOI: 10.1016/j.eneco.2016.02.016.

[18] Juliet Simpson, Eric Loth, and Katherine Dykes. "Cost of Valued Energy for design of renewable energy systems". In: *Renewable Energy* 153 (June 2020), pp. 290–300. ISSN: 18790682. DOI: 10.1016/j.renene.2020.01.131.

[19] H. Canet, A. Guilloré, and C. L. Bottasso. "The eco-conscious wind turbine: design beyond purely economic metrics". In: *Wind Energy Science* 8.6 (2023), pp. 1029–1047. DOI: 10.5194/wes-8-1029-2023.

[20] Rishikesh Joshi, Michiel Kruijff, and Roland Schmehl. "Value-Driven System Design of Utility-Scale Airborne Wind Energy". In: *Energies* 16 (4 Feb. 2023), p. 2075. DOI: 10.3390/en16042075.

[21] Kitepower B.V. *The Hawk - Kitepower.* https://thekitepower.com/the-hawk/. (Accessed on 04/11/2024).

[22] M. Sommerfeld, M. Dörenkämper, J. De Schutter, and C. Crawford. "Scaling effects of fixed-wing ground-generation airborne wind energy systems". In: *Wind Energy Science* 7.5 (2022), pp. 1847–1868. DOI: 10.5194/wes-7-1847-2022. URL: https://wes.copernicus.org/articles/7/1847/2022/.

[23] Rigo Bosman, Valerie Reid, Martin Vlasblom, and Paul Smeets. "Airborne Wind Energy Tethers with High-Modulus Polyethylene Fibers". In: *Airborne Wind Energy. Green Energy and Technology. Springer Berlin Heidelberg.* Ed. by Uwe Ahrens, Moritz Diehl, and Roland Schmehl. 2013, pp. 563–585. DOI: 10.1007/978-3-642-39965-7_33.

[24] R. Joshi, D. von Terzi, M. Kruijff, and R. Schmehl. "Techno-economic analysis of power smoothing solutions for pumping airborne wind energy systems". In: *Journal of Physics: Conference Series* 2265 (2022), p. 042069. ISSN: 1742-6588. DOI: 10.1088/1742-6596/2265/4/042069.

[25] Marco Ghivarello. "KGM1 - A Different Approach to the Airborne Wind Energy Technology". In: *9th international Airborne Wind Energy Conference (AWEC 2021): Book of Abstracts.* http://resolver.tudelft.nl/uuid:f88f2495-34a5-4c32-90c1-a8664f6768a5. Milan, Italy, June 22–24, 2022.

[26] Jannis Heilmann. *The technical and economic potential of Airborne Wind Energy.* Tech. rep. MSC thesis. Utrecht University, 2012.

[27] Frederic Bourgault, Devin Todd, Jason Beatch, Mojtaba Kheiri, Luke Damron, and Vahid Saberi Nasrabad. "Efficient and Power Smoothing Drive-Train Concept for Pumping Kite Generators using Hydraulics". In: *7th international Airborne Wind Energy Conference (AWEC 2017): Book of Abstracts.* https://repository.tudelft.nl/islandora/object/uuid:fba9c248-da91-4252-b89a-d5b6bef124b2/datastream/OBJ/download. Freiburg, Germany, Oct. 5, 2017–Oct. 6, 2022.

[28] Diinef. *Ground stations for Airborne Wind Energy.* https://www.diinef.com/kopi-av-airborne-wind. (Accessed on 04/04/2024).

[29] Luuk van Hagen, Kristian Petrick, Stefan Wilhelm, and Roland Schmehl. "Life-Cycle Assessment of a Multi-Megawatt Airborne Wind Energy System". In: *Energies* 16 (4 Feb. 2023), p. 1750. DOI: 10.3390/en16041750.

[30] Sweder Reuchlin, Rishikesh Joshi, and Roland Schmehl. "Sizing of Hybrid Power Systems for Off-Grid Applications Using Airborne Wind Energy". In: *Energies* 16.10 (May 2023), p. 4036. DOI: 10.3390/en16104036.